Electronic Supplementary Material (ESI) for Nanoscale Horizons.

Supplementary Information

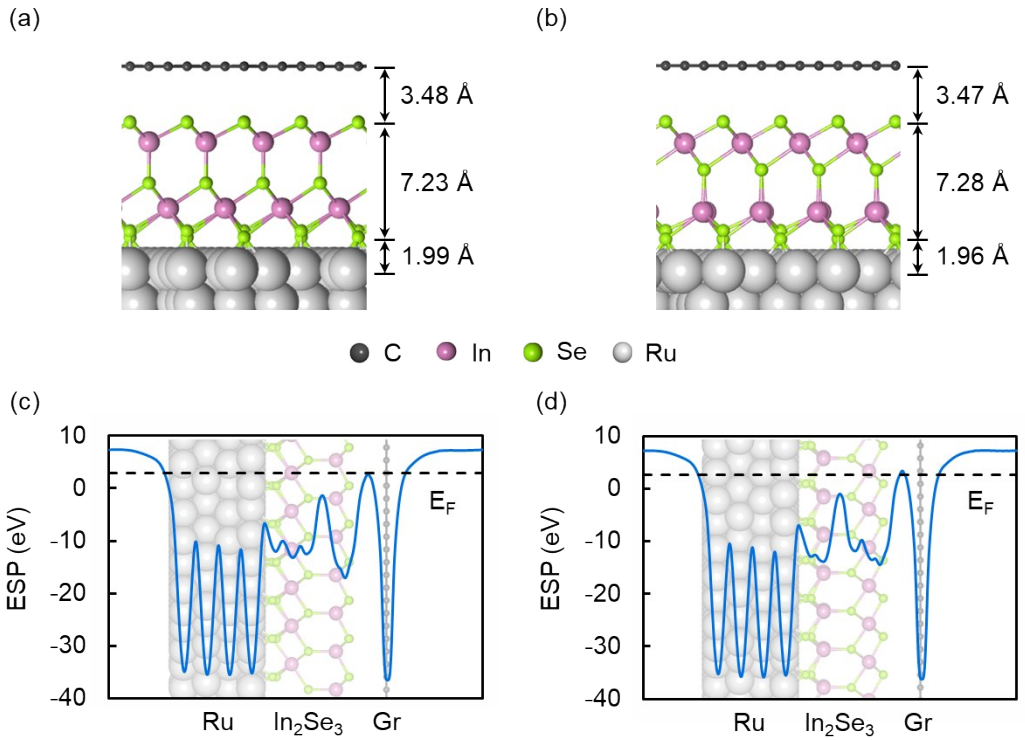

Figure S1. Atomic configurations and plane averaged electrostatic potential of graphene/QL-In_2Se_3/Ru(0001) heterostructure. (a) and (b): Relaxed configurations of a graphene/QL-In_2Se_3/Ru(0001) heterostructure in the two opposite polarizations. The black, purple, green and gray balls represent C, In, Se and Ru atoms, respectively. (c) and (d): Plane-averaged electrostatic potential of (a) and (b), respectively. The horizontal dashed lines represent the Fermi energy (E_F).

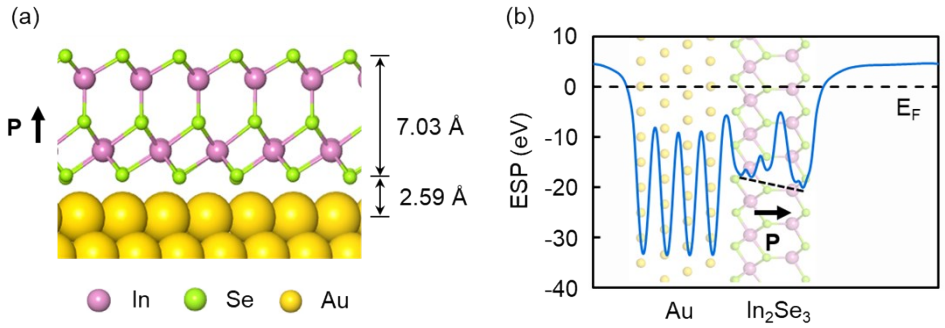

Figure S2. Configuration and plane-averaged electrostatic potential of graphene/1QL-In_2Se_3/Au(111) heterostructure. (a) Relaxed configuration of graphene/1QL-In_2Se_3/Au(111) heterostructure. The distance between the bottom surface of In_2Se_3 and Au is 2.59 Å, which is larger than the typical Au-Se bond length, 2.43~2.48 Å, indicating 1QL-In_2Se_3 is weakly bonded to the Au substrate. (b) Plane-averaged electrostatic potential of (a). The horizontal dashed lines represent the Fermi energy (E_F).

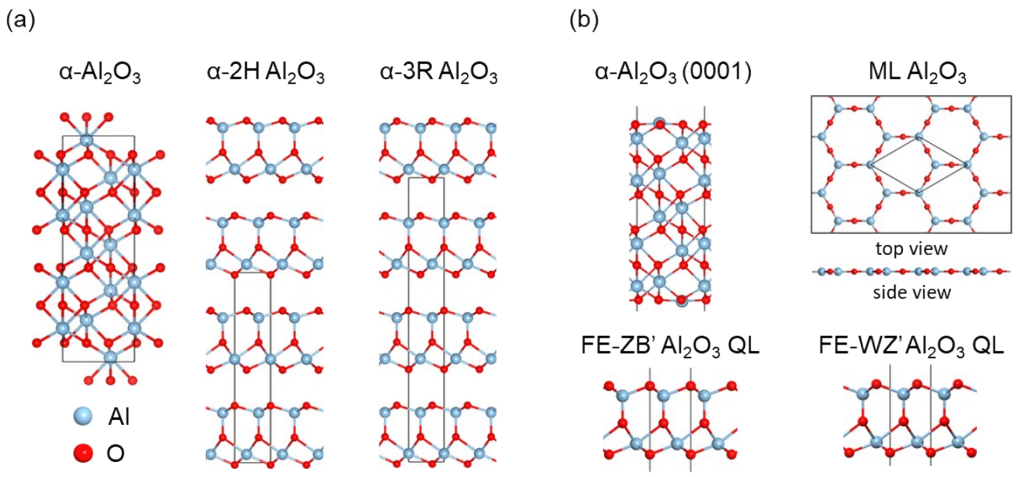

Figure S3. Configurations of bulk Al_2O_3 and freestanding Al_2O_3 layer shown in Table 1. (a) Configurations of α-Al_2O_3 and layered bulk Al_2O_3 comprising QL-Al_2O_3 layers. (b) Configurations of various freestanding Al_2O_3 layers.

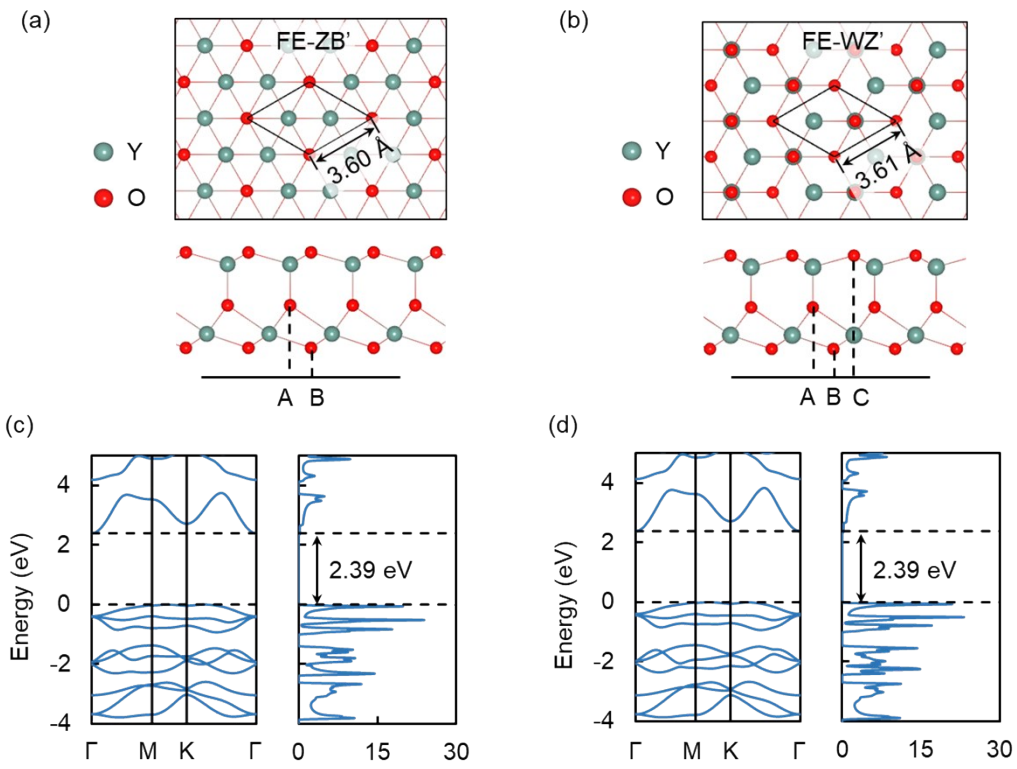

Figure S4. Electronic structures of freestanding QL-Y_2O_3. (a),(b): Top and side views of two phases of freestanding QL-Y_2O_3. O atoms are stacked in A-B and A-B-C sequence in FE-ZB′ and FE-WZ′ respectively. (c),(d): PBE-calculated band structure and DOS of freestanding QL-Y_2O_3 in FE-ZB′ and FE-WZ′ phase, respectively.

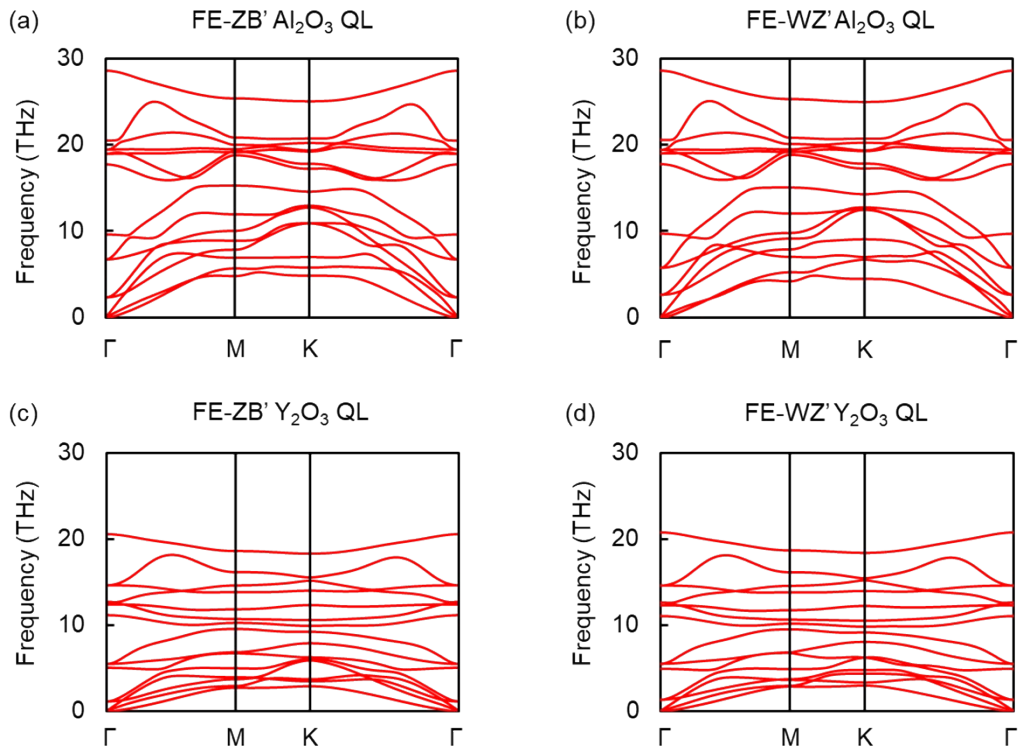

Figure S5. Dynamic stability of QL-M_2O_3 (M=Al, Y). (a), (b) Phonon dispersions of QL-Al_2O_3 in the FE-ZB′ phase and FE-WZ′ phase respectively. The structures have no imaginary-frequency modes. (c), (d) Phonon dispersions of QL-Y_2O_3 in the FE-ZB′ phase and FE-WZ′ phase respectively. The structures have no imaginary-frequency modes.

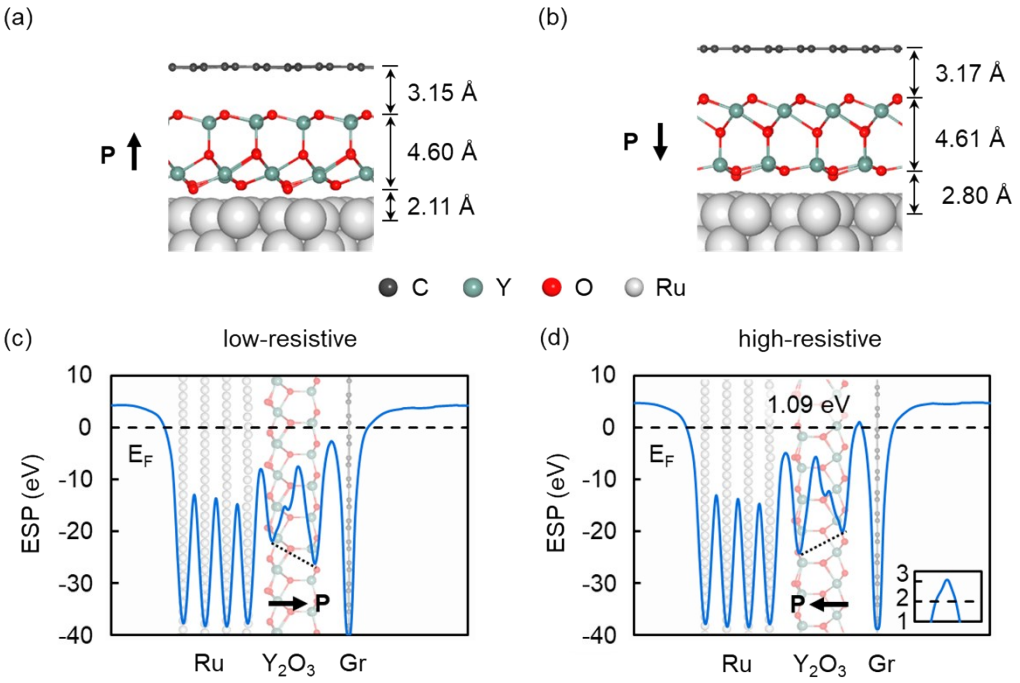

Figure S6. Atomic configurations and plane averaged electrostatic potential of graphene/QL-Y_2O_3/Ru(0001) heterostructure. (a) and (b): Relaxed configurations of graphene/QL-Y_2O_3/Ru(0001) heterostructure with opposite polarizations.. The black, dark green, red, and gray balls represent C, Y, O and Ru atoms respectively. (c) and (d): Plane-averaged electrostatic potential of (a), (b) respectively. The horizontal and sloped dashed lines represent the Fermi energy (E_F) and potential drop across QL-Y_2O_3, respectively. The inset in (d) shows a zoom-in of the potential barrier.

Unlike the case of graphene/QL-Al_2O_3/Ru(0001), in the Y_2O_3 heterostructure the graphene ripples by a very small amount, only 0.12 Å. We have performed calculations using larger, 6 × 6 supercells and the results were essentially unchanged, confirming the smaller ripple.

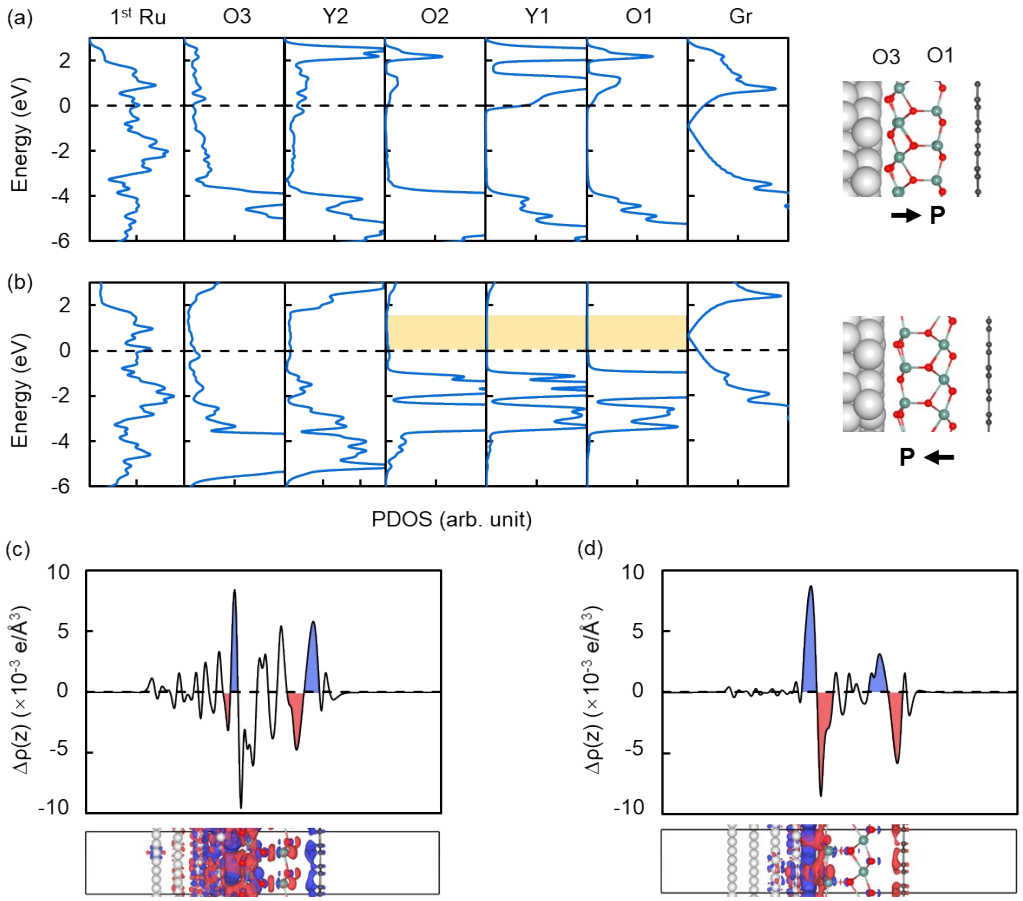

Figure S7. Layer-resolved PDOS and plane-averaged electron density difference of a graphene/QL-Y_2O_3/Ru(0001) heterostructure. (a) and (b): The layer-resolved PDOS of graphene/QL-Y_2O_3/Ru(0001) heterostructures when the polarization points toward and away from graphene, respectively. The tunnel barrier is presented by the yellow region. The Fermi energy is located 0.90 eV above and 0.67 eV below the Dirac point for n- and p-doped graphene. (c) and (d): The plane-averaged charge density difference of the heterostructure. The blue and red region represent electron accumulation and depletion respectively. The isosurface values are set at 0.008 e/Å^3.

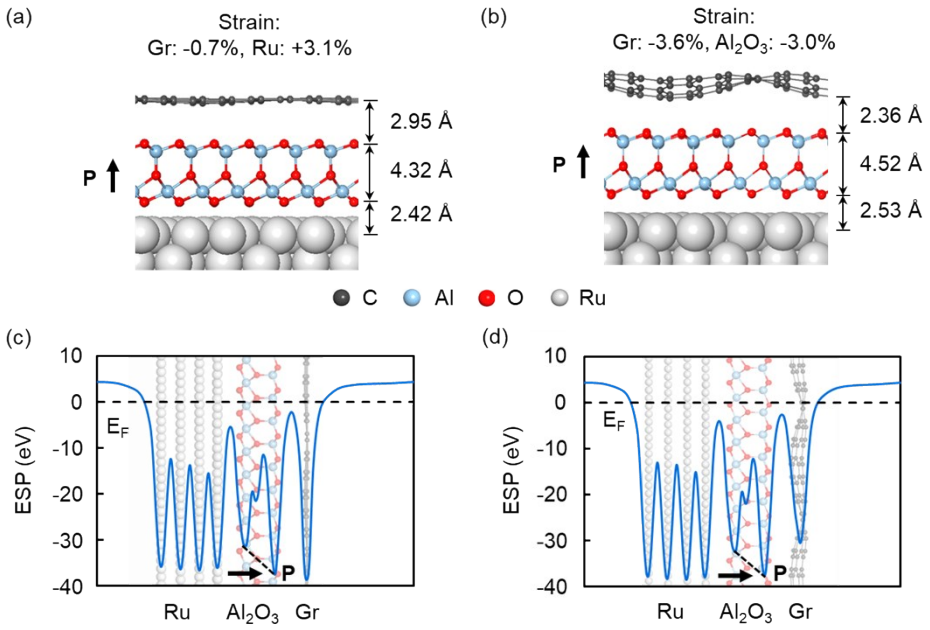

Figure S8. Strain effect on the properties of graphene/QL-Al_2O_3/Ru heterostructure. (a): Relaxed configurations of the new Gr/QL-Al_2O_3/Ru heterostructure, in which QL-Al_2O_3 is unstrained, while graphene and Ru are compressed by 0.7% and stretched by 3.1%, respectively. Strain of Ru was calculated by using the experiment value of the Ru lattice constant. (b): Relaxed configurations of the Gr/QL-Al_2O_3/Ru heterostructure shown in the main text, in which graphene and QL-Al_2O_3 are compressed by 3.6% and 3.0%, respectively, and the lattice constant of Ru(0001) was set to the experimentally measured value. (c) and (d): Plane-averaged electrostatic potential of (a) and (b), respectively.